Current-based design of tensor metasurfaces

Current-Based Design of Tensor Metasurfaces

Lucia Teodorani, Marcello Zucchi, Francesco Lattanzio, and Giuseppe Vecchi
Department of Electronics and Telecommunications, Politecnico di Torino, Turin, Italy, lucia.teodorani@polito.it

***Abstract*—In this work, the design of tensor surface impedances is addressed by adapting a current-based technique for the synthesis of metasurface antennas. An objective function that incorporates both far field and realizability constraints associated with a tensor impedance is minimized using a non-linear conjugate gradient algorithm in order to determine the optimal surface current. From it, the corresponding surface impedance is retrieved and implemented through a suitable selection of anisotropic unit cells. The design of a circular metasurface antenna radiating a squinted beam with linear polarization is demonstrated.**

I. Introduction

In antenna design, metasurfaces, i.e., surfaces inspired by metamaterials and composed of sub-wavelength elements, have become powerful tools to customize and improve antenna functionality because of their unparalleled flexibility in manipulating electromagnetic waves [1].

Due to the design's many degrees of freedom, extremely effective and customized numerical algorithms are needed. An Impedance Boundary Condition (IBC) is used to represent the metasurface for numerical modeling. An anisotropic surface increases radiation efficiency because it provides greater control over surface wave propagation, which lowers side-lobe levels and increases gain [2], [3]; therefore, tensor surface impedances have been the focus of several recently-devised synthesis methods [4], [5].

In this work, the current-based design method for the synthesis of scalar metasurfaces, first introduced in [6] and generalized in [7] to include realistic feeding structures, is extended to deal with the synthesis of tensor surface impedance profiles, while retaining its capability of designing an impedance distribution without any prior knowledge of its shape, and without the need to solve the forward problem at all steps of the algorithm, with a drastic reduction of computational resources, thanks to its current-only approach.

II. Synthesis of Tensor Metasurfaces

The tensor Impedance Boundary Condition (IBC) relates the tangential electric field to the equivalent electric current on the surface:

$$\boldsymbol{E}_{\mathrm{t}}(\boldsymbol{r}) = \overline{\overline{\boldsymbol{Z}}}(\boldsymbol{r}) \cdot \boldsymbol{J}(\boldsymbol{r}). \tag{1}$$

In absence of losses, the impedance is purely reactive; it can be expressed in the Cartesian coordinate basis $(\hat{\boldsymbol{x}}, \hat{\boldsymbol{y}})$ as

$$\overline{\overline{\boldsymbol{Z}}} = \mathrm{j}\begin{bmatrix} X_{xx} & X_{xy} \\ X_{yx} & X_{yy} \end{bmatrix} = \mathrm{j}\begin{bmatrix} X_{\mathrm{I}} + X_{\mathrm{K}} & X_{\mathrm{L}} \\ X_{\mathrm{L}} & X_{\mathrm{I}} - X_{\mathrm{K}} \end{bmatrix} \tag{2}$$

In the above, the term X_{I} corresponds to the *isotropic* part of the tensor, while X_{K} and X_{L} represent the *anisotropy* of the impedance [8].

The electromagnetic scattering problem is formulated as an integral equation (EFIE-IBC),

$$\boldsymbol{E}_{\mathrm{inc}} + \mathcal{L}\boldsymbol{J} = \overline{\overline{\boldsymbol{Z}}} \cdot \boldsymbol{J}, \tag{3}$$

where $\boldsymbol{E}_{\mathrm{inc}}$ is the incident field and $\mathcal{L}$ is the Electric Field Integral Operator. For the numerical discretization the Method of Moments approach with Galerkin testing is employed: the sought current is approximated on a triangular mesh as a linear combination of Rao-Wilton-Glisson (RWG) basis functions [9] defined on the internal mesh edges.

The IBC synthesis is based on the minimization of an objective function that encompasses all the radiated field requirements and impedance realizability constraints:

$$f = f_{\mathrm{rad}} + f_{\mathrm{ibc}}. \tag{4}$$

Here, f_{rad} accounts for the mask-type constraints on the desired radiation pattern, while f_{ibc} expresses the IBC constraints of passivity, losslessness and feasibility range. The computational efficiency of the method, that allows to avoid the solution of the forward problem (3) at every step of the optimization process, stems from expressing all the above functionals, i.e., scalar non-negative functions, as fourth-order polynomials in the current coefficients *only* [6], [7].

The objective function is then minimized using a *non-linear conjugate gradient algorithm*, with a custom line-search procedure that fully exploits the polynomial structure of the objective function. The method is enhanced by using fast numerical algorithms for the computation of the scattered fields from the currents, thus making it suitable to deal with large electromagnetic structures.

Differently from [6], [7], where the design of scalar metasurfaces is tackled, new strategies are needed to:

a) express the tensor impedance components X_{I}, X_{K} and X_{L} as functions of the surface current, and
b) enforce the realizability constraints and impedance bounds, such as those needed to obtain a fully capacitive anisotropic surface, in a tensorial framework.

To this aim, we test (1) with the following independent testing functions, given by the scalar product of three dyadics and the complex conjugate of the current density $\boldsymbol{J}^*$:

$$\boldsymbol{\tau}_{\mathrm{N}} = (\hat{\boldsymbol{y}}\hat{\boldsymbol{x}} - \hat{\boldsymbol{x}}\hat{\boldsymbol{y}}) \cdot \boldsymbol{J}^*, \tag{5}$$

$$\boldsymbol{\tau}_{\mathrm{K}} = (\hat{\boldsymbol{x}}\hat{\boldsymbol{x}} - \hat{\boldsymbol{y}}\hat{\boldsymbol{y}}) \cdot \boldsymbol{J}^*, \tag{6}$$

$$\boldsymbol{\tau}_{\mathrm{L}} = (\hat{\boldsymbol{y}}\hat{\boldsymbol{x}} + \hat{\boldsymbol{x}}\hat{\boldsymbol{y}}) \cdot \boldsymbol{J}^*. \tag{7}$$

After some manipulations, we obtain a diagonal linear system,

$$\begin{bmatrix} -\mathcal{J}_{\mathrm{N}} & 0 & 0 \\ 0 & -\mathcal{J}_{\mathrm{N}} & 0 \\ 0 & 0 & \mathcal{J}_{\mathrm{N}} \end{bmatrix} \begin{bmatrix} X_{\mathrm{I}} \\ X_{\mathrm{K}} \\ X_{\mathrm{L}} \end{bmatrix} = \begin{bmatrix} P_{\mathrm{N}} \\ P_{\mathrm{L}} \\ P_{\mathrm{K}} \end{bmatrix}, \tag{8}$$

whose terms are defined as

$$\mathcal{J}_{\rm N} = -\operatorname{Im}\left(\boldsymbol{\tau}_{\rm N}\cdot\boldsymbol{J}\right), \qquad P_{\rm N} = -\operatorname{Re}\left(\boldsymbol{\tau}_{\rm N}\cdot\boldsymbol{E}\right)$$
$$P_{\rm L} = \operatorname{Re}\left(\boldsymbol{\tau}_{\rm L}\cdot\boldsymbol{E}\right), \qquad P_{\rm K} = \operatorname{Re}\left(\boldsymbol{\tau}_{\rm K}\cdot\boldsymbol{E}\right).$$

The solution of (8) is then given by

$$X_{\rm I} = -P_{\rm N}/\mathcal{J}_{\rm N}, \tag{9}$$
$$X_{\rm K} = -P_{\rm L}/\mathcal{J}_{\rm N}, \tag{10}$$
$$X_{\rm L} = P_{\rm K}/\mathcal{J}_{\rm N}. \tag{11}$$

Regarding the enforcement of realizability constraints, it can be shown that capacitive or inductive behavior is expressed by the sign of the eigenvalues the tensor (2):

$$X_1 = X_{\rm I} + \sqrt{X_{\rm K}^2 + X_{\rm L}^2}, \tag{12}$$
$$X_2 = X_{\rm I} - \sqrt{X_{\rm K}^2 + X_{\rm L}^2}. \tag{13}$$

Hence, enforcing unit cells of either type requires enforcing the sign of the eigenvalues. In the design of practically relevant metasurface antennas, we are usually interested in capacitive impedances, that can be easily implemented with patterned metallic patches on the dielectric substrate; this condition is enforced by requiring both eigenvalues of the tensor to be negative, as in

$$X_{\rm I} < 0, \tag{14}$$
$$X_{\rm I}^2 > X_{\rm K}^2 + X_{\rm L}^2. \tag{15}$$

By substituting (9)–(11) in (14)–(15), we can define all constraints in terms of the surface current only, and the associated cost functionals can be included in the current-based optimization in a straightforward way.

Finally, the synthesis process requires the derivation of the proper metallic patterning of each cell in the lattice from the computed tensor impedance values. This is done by picking a suitable candidate from a database of pre-computed geometries, where each shape is simulated within a periodic environment and its impedance is extracted from normal-incidence scattering simulations [10].

III. Results

A circular metasurface antenna radiating a linearly-polarized squinted beam towards $(\theta, \varphi) = (30^\circ, 60^\circ)$ has been designed at a frequency of $23\,\mathrm{GHz}$. A RO3003 dielectric substrate with $\varepsilon_r = 3$ and thickness $1.27\,\mathrm{mm}$ is chosen. The antenna has a radius of $6\,\lambda_0$ at the working frequency, for a diameter of $156\,\mathrm{mm}$. The feeding structure consists of a vertical central pin, fed through an aperture in the ground plane, and an annular ring that ensures good matching with the metasurface; these metallic elements have been self-consistently accounted for in the optimization process as illustrated in [7]. The complete antenna is discretized with $N = 44\,244$ RWG basis functions.

The upper bound for $X_{\rm I}$ is set equal to $-400\,\Omega$; this value derives from the analysis of the data set of a double-anchor unit cell of size $1/8\,\lambda_0$ (not reported here). The desired squinted beam has linear polarization along $\hat{\boldsymbol{x}}$, with sidelobes levels below $-20\,\mathrm{dB}$.

Figures 1a–1c show the synthesized tensor coefficients $X_{\rm I}$, $X_{\rm K}$, $X_{\rm L}$, while Figs. 1d–1f show the same profile expressed in Cartesian coordinates. The isotropic coefficient values are below the set upper bound. Observing the eigenvalues distributions in Figs. 2a and 2b, it is clear that the synthesize impedance is capacitive over the entire surface, since both X_1 and X_1 are negative everywhere.

The resulting realized gain pattern is shown in Fig. 3, together with the surface current magnitude. Both the co- and cross-polarization components comply with the requirements, with a maximum realized gain of 26 dB.

IV. Conclusions

In this work, a current-based method for the synthesis of tensor metasurface antennas has been described. By using a suitable local testing approach, the tensor impedance distribution can be obtained from the optimum current. The proposed algorithm has been used to design a MTS antenna radiating a linearly-polarized squinted beam. The eigenvalues distribution shows that the resulting impedance satisfies all condition for a capacitive impedance profile.

Acknowledgement

This work was supported by the European Union - Next Generation EU under the Italian National Recovery and Resilience Plan (NRRP), Mission 4, Component 2, Investment 1.3, CUP E13C22001870001, partnership on "Telecommunications of the Future" (PE00000001 - program "RESTART").

References

[1] M. Faenzi, G. Minatti, D. González-Ovejero, F. Caminita, E. Martini, C. Della Giovampaola, and S. Maci, "Metasurface Antennas: New Models, Applications and Realizations," *Sci. Rep.*, vol. 9, no. 1, p. 10178, Dec. 2019.

[2] G. Minatti, M. Faenzi, E. Martini, F. Caminita, P. De Vita, D. Gonzalez-Ovejero, M. Sabbadini, and S. Maci, "Modulated Metasurface Antennas for Space: Synthesis, Analysis and Realizations," *IEEE Trans. Antennas Propag.*, vol. 63, no. 4, pp. 1288–1300, Apr. 2015.

[3] G. Minatti, F. Caminita, E. Martini, M. Sabbadini, and S. Maci, "Synthesis of Modulated-Metasurface Antennas With Amplitude, Phase, and Polarization Control," *IEEE Trans. Antennas Propag.*, vol. 64, no. 9, pp. 3907–3919, Sep. 2016.

[4] M. Bodehou, C. Craeye, E. Martini, and I. Huynen, "A Quasi-Direct Method for the Surface Impedance Design of Modulated Metasurface Antennas," *IEEE Trans. Antennas Propag.*, vol. 67, no. 1, pp. 24–36, Jan. 2019.

[5] S. Pearson and S. V. Hum, "Optimization of Electromagnetic Metasurface Parameters Satisfying Far-Field Criteria," *IEEE Trans. Antennas Propag.*, vol. 70, no. 5, pp. 3477–3488, May 2022.

[6] M. Zucchi, F. Vernì, M. Righero, and G. Vecchi, "Current Based Automated Design of Realizable Metasurface Antennas With Arbitrary Pattern Constraints," *IEEE Trans. Antennas Propag.*, vol. 71, no. 6, pp. 4888–4902, Jun. 2023.

[7] L. Teodorani, M. Zucchi, and G. Vecchi, "Generalized Deterministic Automated Design of Metasurface Antennas With 3-D Feeding Structures," *IEEE Trans. Antennas Propag.*, vol. 72, no. 11, pp. 8135–8150, Nov. 2024.

[8] I. Lindell, A. Sihvola, and I. Hänninen, "Perfectly anisotropic impedance boundary," *IET Microw. Antennas Propag.*, vol. 1, no. 3, p. 561, 2007.

[9] S. Rao, D. Wilton, and A. Glisson, "Electromagnetic scattering by surfaces of arbitrary shape," *IEEE Trans. Antennas Propag.*, vol. 30, no. 3, pp. 409–418, May 1982.

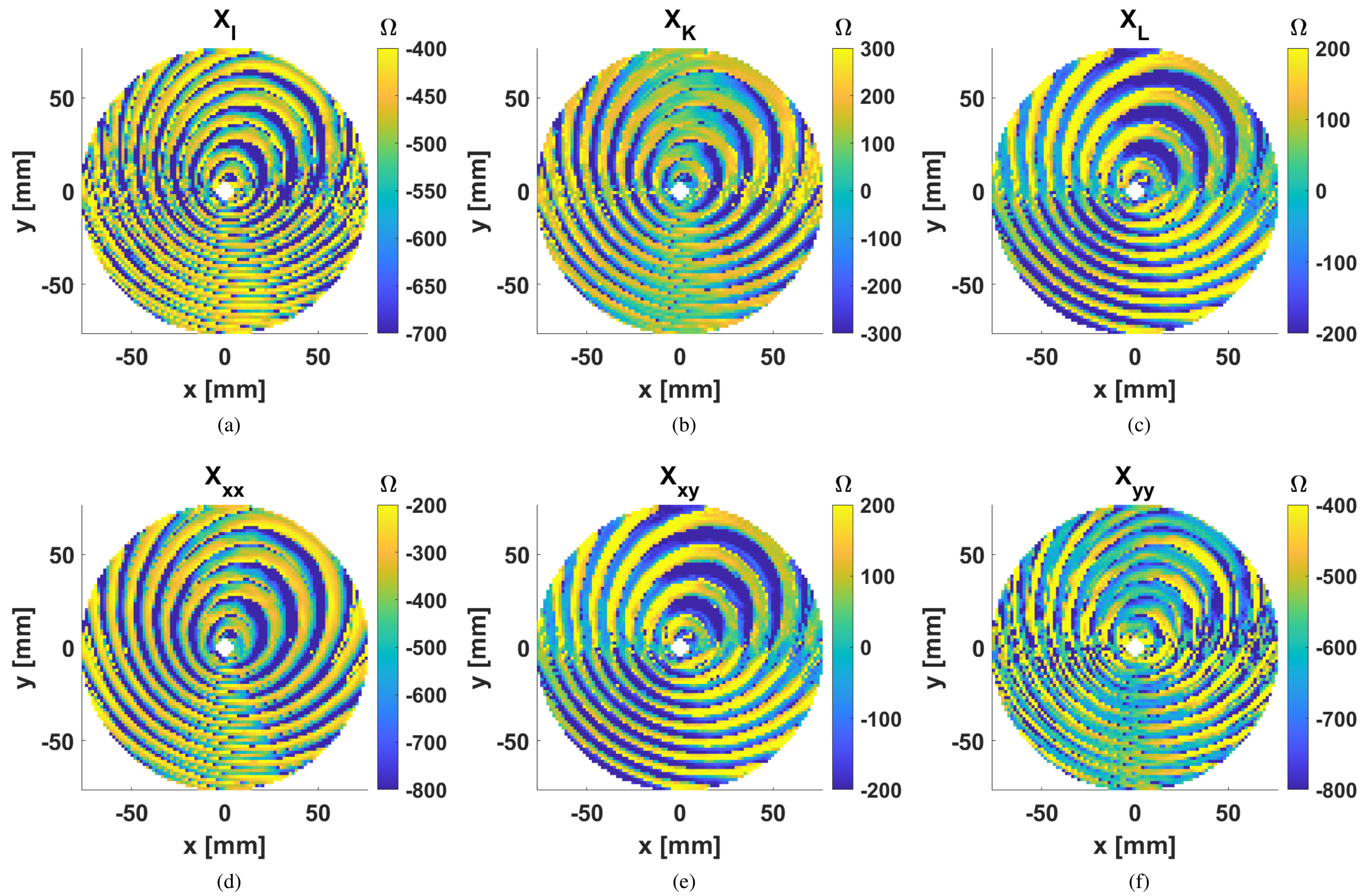

Fig. 1. Circular tensor MTS antenna radiating a linearly-polarized squinted beam: (a), (b) and (c) synthesized surface tensor parameters, (d), (e) and (f) corresponding surface tensor components in Cartesian coordinates.

[10] A. M. Patel and A. Grbic, "Effective Surface Impedance of a Printed-Circuit Tensor Impedance Surface (PCTIS)," *IEEE Trans. Microw. Theory Tech.*, vol. 61, no. 4, pp. 1403–1413, Apr. 2013.

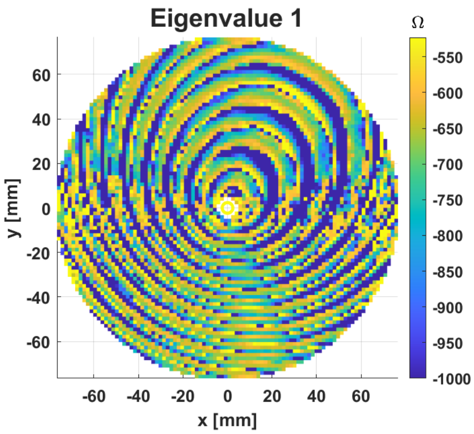

(a)

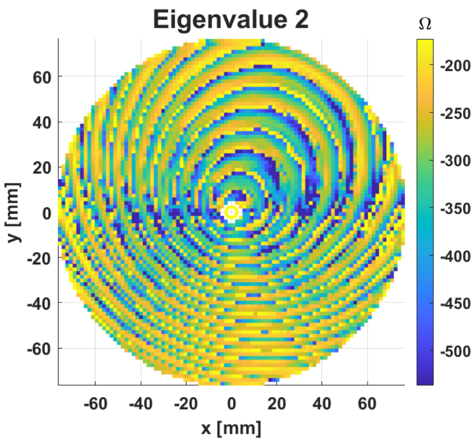

(b)

Fig. 2. Eigenvalues (a) X_1 and (b) X_2 of the synthesized surface tensor impedance.

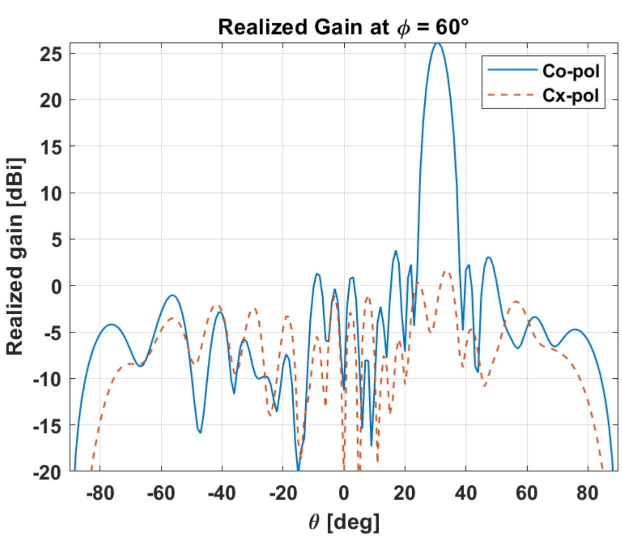

Fig. 3. Far field realized gain pattern for co-polar (*blue*) and cross-polar (*red*) in the plane $\varphi = 60°$.